2024 IEEE 10th International Power Electronics and Motion Control Conference (IPEMC2024-ECCE Asia) | 979-8-3503-5133-0/24/$31.00 ©2024 IEEE | DOI: 10.1109/IPEMC-ECCEAsia60879.2024.10567066

A Current Sensorless Model Predictive Current Control Method With Luenberger Observer For PMSM Drives

1st Sicong Wen
School of Automation
Northwestern Polytechnical University
Xi'an, China
sicongwen@mail.nwpu.edu.cn

2nd ManFeng Dou
School of Automation
Northwestern Polytechnical University
Xi'an, China
doumf@nwpu.edu.cn

3rd Dongdong Zhao
School of Automation
Northwestern Polytechnical University)
Xi'an, China
zhaodong@nwpu.edu.cn

4th Zhiguang Hua
School of Automation
Northwestern Polytechnical University
Xi'an, China
zhiguang.hua@nwpu.edu.cn

***Abstract*—Extensive research has been conducted on the permanent magnet synchronous motor (PMSM) in recent years. In the event of current sensors failure, PMSM operation is greatly affected. In this article, The current sensorless speed control for PMSM is implemented using Model Predictive Current Control (MPCC) as the controller. A current sensorless MPCC based on the Luenberger observer is presented for PMSM drives. The method consists of dq-axis current estimation using only position sensors. The motion equation is used to obtain the q-axis current. Besides, The three-phase system's currents are observed using a Luenberger observer in the abc reference frame. Moreover, the d-axis current is obtained using the estimated three-phase currents. Actual speed and estimated current of the dq-axis are applied to MPCC for PMSM drives. Simulations confirm that the suggested approach works.**

***Index Terms*—current sensorless, MPCC, PMSM, Luenberger observer**

I. Introduction

Due to its high torque density, exceptional maintainability, and other notable attributes, the Permanent Magnet Synchronous Motor (PMSM) finds widespread application in precision machining and robotic endeavors. [1]. As the application scope of PMSM continues to expand, the requirements for control performance are becoming more precise. Model predictive current control (MPCC) has garnered significant attention in the domain of electrical power systems and motor control applications, attributed to its high dynamic performance and simplicity in addressing multiple objectives [2]. However, MPCC relies on the current sensor to get real-time current to predict the next sampling time current. PMSM drives may fail due to strong thermal stress and electromagnetic under changing operating conditions [3]. The current sensor faults can cause unacceptable deterioration of drive performance. Therefore, the control technology of the current sensorless is of great importance to make the motor run normally and realize fault tolerance. In recent years, some studies on current sensorless control have been presented. Based extended Kalman filter, an estimated current method was proposed [4]. A Model-Free-Control (MFC) method was presented, which only used measured rotor mechanical speed and input filter voltage [5]. A drive system was devised which omits current sensors and relies solely on a resolution position sensor for operation. [6]. A method utilizing a single speed controller for direct voltage control of interior PMSM was proposed, while no current sensor is needed [7]. A fault-tolerant control (FTC) approach for current sensors, based on a sliding mode observer (SMO), was introduced, which can achieve rotor position estimation and current error constructuon [8]. A current reconstruction approach using a single estimator, rotor speed, and DC link voltage is proposed [9].

A novel MPCC based on the Luenberger current observer is designed, which can achieve high performance operation of PMSM with only the position sensor. The q-axis current is derived by utilizing the motion equation of PMSM. Furthermore, the Luenberger observer is established to estimate the three-phase current in the abc reference frame, which undergoes Clark and Park transform to obtain the d-axis current. Finally, the estimated currents are adopted in MPCC to generate the optimal switching states, which directly drive the inverter. The proposed controller's effectiveness is verified through simulation results.

II. Model Predictive Current Control and Proposed Method

A. MPCC based on current sensor

The PMSM is represented in the synchronous dq frame by the following equation:

979-8-3503-5133-0/24/$31.00 ©2024 IEEE

$$\begin{cases} u_d = R_s i_d + L_s \frac{di_d}{dt} - \omega_e L_s i_q \\ u_q = R_s i_q + L_s \frac{di_q}{dt} + \omega_e (L_s i_d + \psi_f) \end{cases} \quad (1)$$

u_d and u_q respectively represent the voltage of the dq-axis. On the other hand, R_s symbolizes the electrical resistance, while L_s signifies the magnitude of stator inductance, i_d and i_q respectively represent the current of the dq-axis. ω_e represent the electrical angular velocity of the motor, while $\psi_f$denotes the magnetic flux linkage of the permanent magnet.

$$T_e = \frac{3}{2} p \psi_f i_q \quad (2)$$

where T_e represents the motor torque, and *p* denotes the pole pair of the PMSM. The motion formula for PMSM is as stated below

$$p\omega_e = \frac{1}{J}(T_e - T_L) - \frac{1}{J} B \omega_e \quad (3)$$

where *J* and *B* represent the inertia of the drive and static friction of the PMSM respectively, T_L denotes the load torque.

By rewriting equation (1) , we can establish the state representation for the stator current in the subsequent manner.

$$\begin{cases} \frac{di_d}{dt} = -\frac{R_s}{L_s} i_d + \frac{1}{L_s}(u_d + \omega_e L_s i_q) \\ \frac{di_q}{dt} = -\frac{R_s}{L_s} i_q + \frac{1}{L_s}(u_q - \omega_e (L_s i_d + \psi_f)) \end{cases} \quad (4)$$

Employing the first-order Euler discretization technique to approximate the equation (4), we can forecast the stator current at the subsequent sampling time.

$$\begin{cases} i_d(k+1) = (1 - T_s R_s L_s^{-1}) i_d(k) \\ + T_s L_s^{-1} R_s u_d(k) + T_s \omega_e(k) i_q(k) \\ i_q(k+1) = (1 - T_s R_s L_s^{-1}) i_q(k) \\ + T_s L_s^{-1} u_q(k) - T_s \omega_e(k)(L_s i_d(k) + \psi_f) \end{cases} \quad (5)$$

where T_s is the sampling time, $i_d q(k+1)$ refer to the current of *dq*-axis at *k*+1 time.

The cost function *J* is typically constructed to assess performance across various voltage vectors, as outlined below.

$$J = \left| i_d^{ref} - i_d(k+1) \right| + \left| i_q^{ref} - i_q(k+1) \right| \quad (6)$$

where i_d^{ref} and i_q^{ref} is reference current.

The block diagram depicting the control structure of traditional MPCC, which relies on current sensors, is presented in Figure 1.

Capturing the three-phase current at time *k* using the current sensor is crucial for accurately forecasting the next stator current. The MPCC relies on both the position sensor and current sensors. If current sensors fail or have a large error, the performance of MPCC will deteriorate. To overcome this potential issue, this paper puts forward a novel MPCC method, which current sensorless.

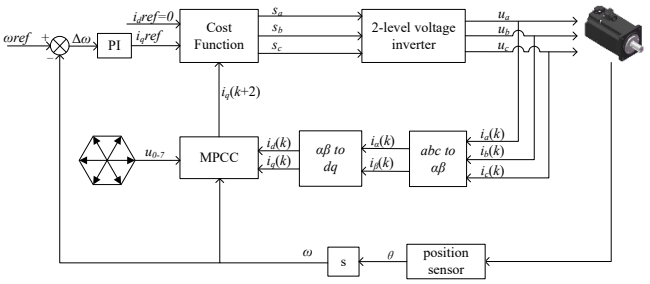

Fig. 1. Block diagram for MPCC with current sensor

B. Suggested approach

In order to solve the issue above-mentioned, substituting the equation (2) into the equation (3)

$$i_q(k) = \frac{2}{3}\left(\frac{B}{p_0 \psi_f}\omega_e(k) + \frac{J}{p_0 \psi_f} p\omega_e(k) + \frac{1}{p_0 \psi_f} T_L\right) \quad (7)$$

The relationship between the stator voltage and current in stationary *abc* frame is shown by

$$\begin{cases} u_a = R_s i_a + p\psi_a \\ u_b = R_s i_b + p\psi_b \end{cases} \quad (8)$$

i_c can be obtained by

$$i_c = -i_a - i_b \quad (9)$$

where $\psi_a b$ and ψ_b represent the components of ψ_s along the *ab*-axis. ψ_a and ψ_b can be obtained by

$$\begin{cases} \psi_a = \psi_f \cos\theta_e + L_s i_a \\ \psi_b = \psi_f \cos(\theta_e - \frac{2\pi}{3}) + L_s i_b \end{cases} \quad (10)$$

The symbol θ_e stands for the electrical angle of the rotor. Substituting equation (10) into (8)

$$\begin{cases} L_s p i_a + R_s i_a - \psi_f \omega_e \sin\theta_e = u_a \\ L_s p i_b + R_s i_b - \psi_f \omega_e \sin(\theta_e - \frac{2\pi}{3}) = u_b \end{cases} \quad (11)$$

Using the equation (9), the *Clark* and *Park* transform, the relationship of i_q and i_a and i_b is shown by

$$\begin{bmatrix} i_d \\ i_q \end{bmatrix} = \frac{2}{3} \begin{bmatrix} \sqrt{3}\cos(\theta_e - \frac{\pi}{6}) & \sqrt{3}\sin\theta_e \\ \sqrt{3}\cos(\theta_e + \frac{\pi}{3}) & \sqrt{3}\cos\theta_e \end{bmatrix} \begin{bmatrix} i_a \\ i_b \end{bmatrix} \quad (12)$$

By using equation (11) and (12) , Luenberger observer is established as follows

$$\begin{cases} \hat{\dot{x}} = A\hat{x} + B + L(i_q - \hat{i}_q) \\ \hat{i}_q = Cx \end{cases} \quad (13)$$

where

$$
\begin{cases}
x = \begin{bmatrix} i_a & i_b \end{bmatrix}^T \\
A = \begin{bmatrix} \frac{-R_S}{L_s} & 0 \\ 0 & \frac{-R_S}{L_s} \end{bmatrix} \\
B = \begin{bmatrix} \frac{\psi_f \sin\theta_e \omega_e}{L_s} + \frac{u_a}{L_s} \\ \frac{\psi_f \sin(\theta_e - \frac{2\pi}{3})\omega_e}{L_s} + \frac{u_b}{L_s} \end{bmatrix} \\
C = \begin{bmatrix} \sqrt{3}\cos(\theta_e + \frac{\pi}{3}) & \sqrt{3}\cos\theta_e \end{bmatrix} \\
L = \begin{bmatrix} L_1 & L_2 \end{bmatrix}^T
\end{cases} \tag{14}
$$

By adjusting the value of L, x will converge to its actual value. By using the equation (12), i_d can be obtained.

The diagrammatic representation of the control block for the proposed method, which relies on a sensorless current approach, is illustrated in Figure 2.

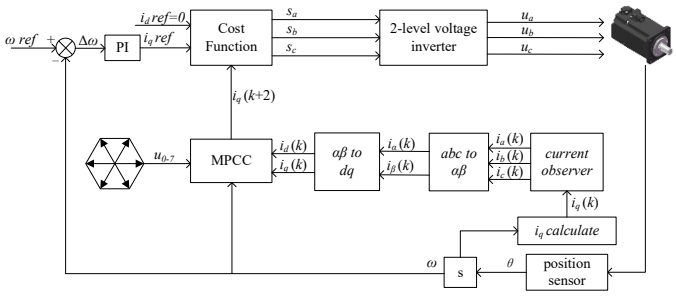

Fig. 2. Block diagram for MPCC based on current sensorless

C. Convergence Analysis

The following equation can be derived using equation (13)

$$\dot{\hat{x}} = (A - LC)\hat{x} + B + Li_q \tag{15}$$

Let $e = x - \hat{x}$ and $\dot{e} = \dot{x} - \dot{\hat{x}}$. Based on equations (11) , (12) and (15), the derivation of the error equation proceeds as follows.

$$\dot{e} = (A - LC)e \tag{16}$$

According to equation(16), the characteristic equation can be derived as

$$|s - A + LC| = (s + \frac{R_s}{L_s})(s + \frac{R_s}{L_s} + \sqrt{3}l_1 \cos(\theta_e + \frac{\pi}{3}) + \sqrt{3}l_2 \cos\theta_e) \tag{17}$$

According to equation(17), properly setting l_1 and l_2 can ensure that the characteristic root has a negative real part and the observation error will converge to 0.

III. SIMULATION RESULTS

Simulation experiments were conducted to validate the performance of the proposed controller, with the motor parameters outlined in TABLE I.

With the load torque kept constant at 0, the motor gradually accelerates from 0 to 1000 revolutions per minute, the simulation experimental waveforms of observed i_a and the actual i_a are shown in Fig. 3.

TABLE I
PARAMETERS OF THE TESTED PMSM

Parameter	Symbol	Value
Driving voltage	U_{dc}	24 V
Resistance	R_s	0.03
Armature inductance	L_s	0.15 mH
Flux linkage	ψ_f	0.008 Wb
Viscous damping	B	0.0004924 (Nms)
Inertia	J	0.00426 (kg.m^2)
Pole pairs	p	5

The observed current i_a coincides with the true current i_a under a load torque of 0, as depicted in Fig. 3. The proposed current observer can obtain the observed current well. A

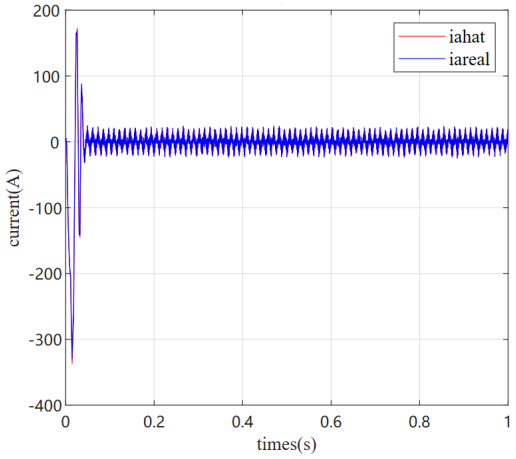

Fig. 3. observed i_a and actual i_a of the proposed approach while torque is 0

similar result is found for the observed current i_b as shown in Fig. 4. This proves that the proposed observer can converge quickly.

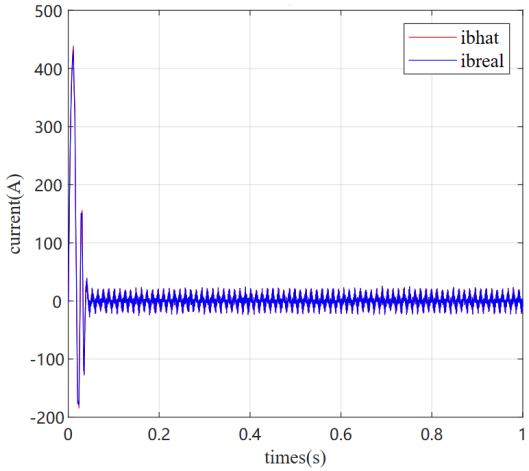

Fig. 4. observed i_b and actual i_b of the proposed approach while torque is 0 Nm

Upon reaching a load torque of 0.5 Nm, the observed current of the observer is still aligns closely with the actual current, indicating the effectiveness of the observer, as depicted in Fig.5 and Fig. 6.

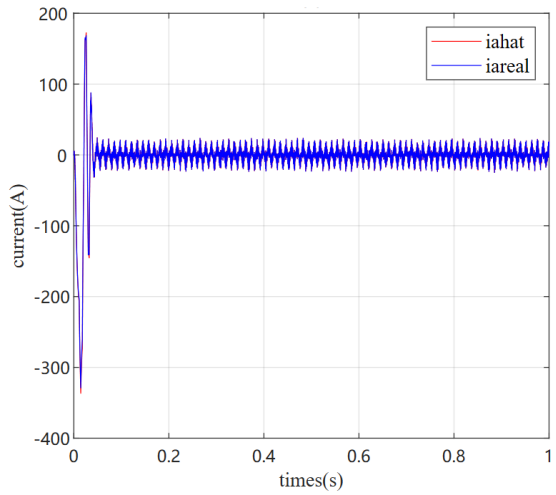

Fig. 5. observed i_a and actual i_a of the proposed approach while torque is 0.5 Nm

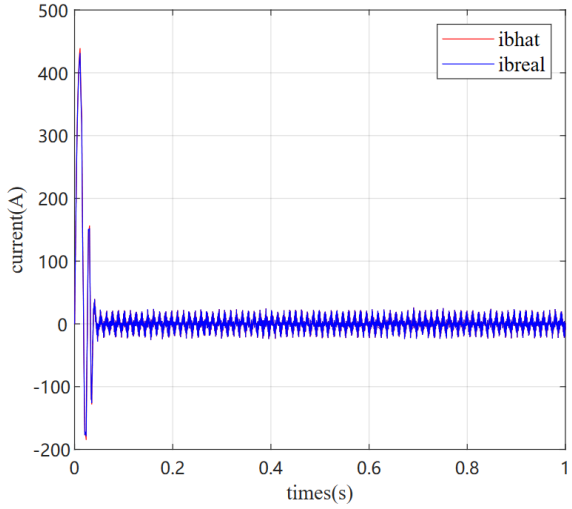

Fig. 6. observed i_b and actual i_b of the proposed approach while torque is 0.5 Nm

Compared with traditional MPCC based on the current sensor, the speed response of the proposed approach is similar to the traditional approach from Fig. 7.

However, the torque fluctuation of proposed approach is slightly greater compared to that of the conventional method from Fig. 8

As the load torque increases to 1 Nm, it can be observed from the Fig. 9 that both the traditional MPCC method and the MPCC method without current sensor achieve the reference value.

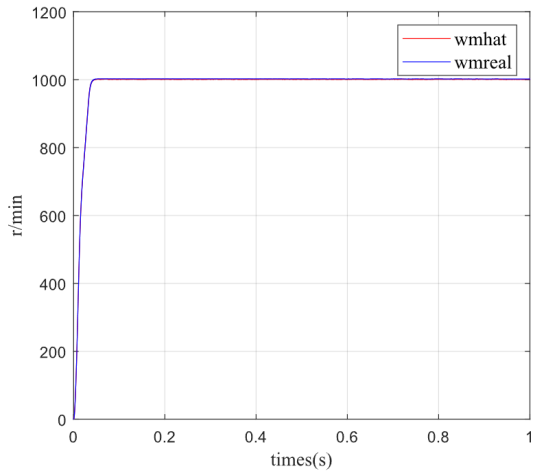

Fig. 7. A comparison of speeds is made between the introduced method and the conventional MPCC, with torque set at 0 Nm.

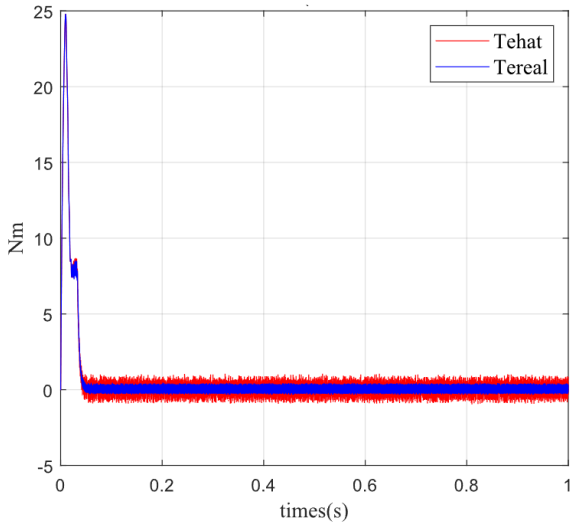

Fig. 8. A comparison of torques is conducted between the introduced approach and the conventional MPCC, with the torque maintained at 0 Nm.

However, the torque of the MPCC method without current sensor is relatively large from Fig. 10.

When the current suddenly fails at 0.5s, the system continues to run using the observed current value. According to the depictions in Fig. 11 and Fig. 12, the speed has a small speed drop and the electromagnetic torque fluctuation becomes larger, but the motor can still run smoothly.

Through the above simulation verification, the effectiveness of the current observer is confirmed. It demonstrates that the motor can maintain stable operation even upon occurrence of current sensor malfunction, even if the electromagnetic torque fluctuation becomes larger.

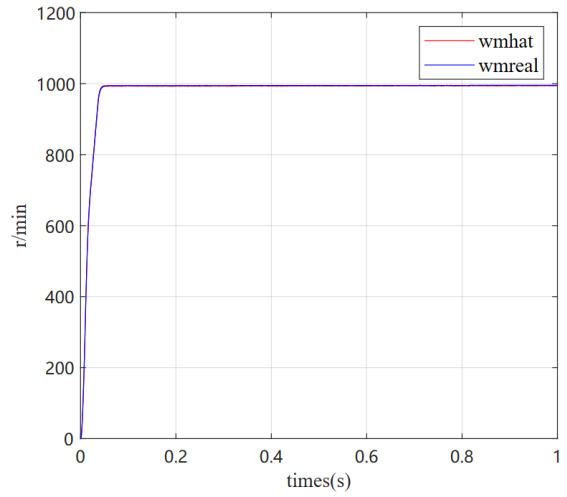

Fig. 9. A comparative analysis is conducted to assess the speed of the presented methodology in comparison to the conventional MPCC, utilizing a torque setting of 1 Nm.

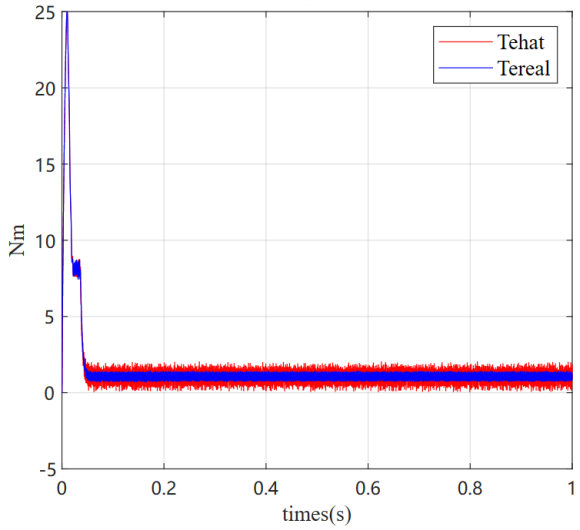

Fig. 10. A comparative analysis is conducted to assess the torque of the presented methodology in comparison to the conventional MPCC, utilizing a torque setting of 1 Nm.

IV. CONCLUSIONS

To improve the robustness of PMSM with current sensor fault, a current sensorless MPCC method based on the Luenberger observer was proposed in this article. The simulation results indicate that the responsive characteristics of the proposed method resembled those of the traditional approach which had three-phase current sensors, but the fluctuation of torque was relatively large. Upcoming research will be directed towards compensating the system for disturbance to enhance the accuracy of current estimation and suppress torque ripple effects.

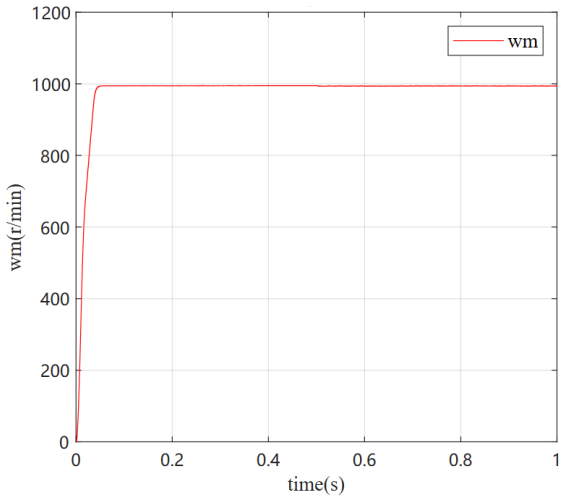

Fig. 11. Speed of PMSM running state, when 0.5s current sensor failure

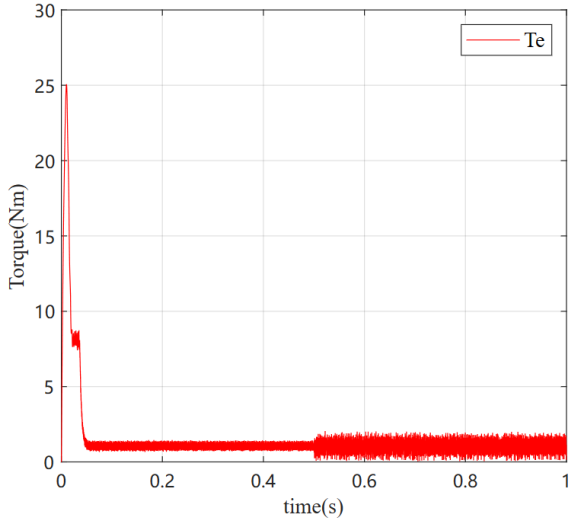

Fig. 12. Torque of PMSM running state, when 0.5s current sensor failure

ACKNOWLEDGMENT

This work was supported in part by the National Natural Science Foundation of China (No. 52307251, No.52277226) and the China Postdoctoral Science Foundation (No.2023TQ0277, No. 2023M742840).

REFERENCES

[1] X. Liu, H. Chen, J. Zhao and A. Belahcen, "Research on the Performances and Parameters of Interior PMSM Used for Electric Vehicles," in IEEE Transactions on Industrial Electronics, vol. 63, no. 6, pp. 3533-3545, June 2016.

[2] Y. Wei, D. Ke, H. Qi, F. Wang and J. Rodríguez, "Multistep Predictive Current Control for Electrical Drives With Adaptive Horizons," in IEEE Transactions on Industrial Electronics, vol. 71, no. 1, pp. 250-260, Jan. 2024.

[3] G. Ma, H. Zhang, Z. Sun, C. Yao, G. Ren and S. Xu, "Current Sensor Fault Localization and Identification of PMSM Drives Using Difference Operator," in IEEE Journal of Emerging and Selected Topics in Power Electronics, vol. 11, no. 1, pp. 1097-1110, Feb. 2023.

[4] Y. Li, M. Yang, J. Long, Z. Liu and D. Xu, "Current sensorless predictive control based on extended kalman filter for pmsm drives," 2017 IEEE Transportation Electrification Conference and Expo, Asia-Pacific (ITEC Asia-Pacific), Harbin, China, 2017, pp. 1-6.
[5] S. A. Hashjin, E. -H. Miliani, K. Ait-Abderrahirrr and B. Nahid-Mobarakeh, "Current Sensorless Model Free Control Applied on PMSM Drive System," 2019 IEEE Transportation Electrification Conference and Expo (ITEC), Detroit, MI, USA, 2019, pp. 1-5.
[6] S. Morimoto, M. Sanada and Y. Takeda, "High-performance current-sensorless drive for PMSM and SynRM with only low-resolution position sensor," in IEEE Transactions on Industry Applications, vol. 39, no. 3, pp. 792-801, May-June 2003.
[7] M. Khayamy and H. Chaoui, "Current Sensorless MTPA Operation of Interior PMSM Drives for Vehicular Applications," in IEEE Transactions on Vehicular Technology, vol. 67, no. 8, pp. 6872-6881, Aug. 2018.
[8] G. Wang, X. Hao, N. Zhao, G. Zhang and D. Xu, "Current Sensor Fault-Tolerant Control Strategy for Encoderless PMSM Drives Based on Single Sliding Mode Observer," in IEEE Transactions on Transportation Electrification, vol. 6, no. 2, pp. 679-689, June 2020.
[9] Y. Azzoug, M. Sahraoui, R. Pusca, T. Ameid, R. Romary and A. J. M. Cardoso, "A Variable Speed Control of Permanent Magnet Synchronous Motor Without Current Sensors," 2020 IEEE 29th International Symposium on Industrial Electronics (ISIE), Delft, Netherlands, 2020.